Synthesis of Aqueous Polyethylene Dispersions with Electron-Deficient Neutral Nickel(II) Catalysts with Enolatoimine Ligands

Sze-Man Yu, Andreas Berkefeld, Inigo Göttker-Schnetmann, Gerhard Müller, and Stefan Mecking*

Universität Konstanz, Lehrstuhl für Chemische Materialwissenschaft, Fachbereich Chemie, Universitätsstr. 10, D-78457 Konstanz, Germany

Received August 8, 2006; Revised Manuscript Received November 3, 2006

ABSTRACT: A series of new, electron-poor neutral κ^2-N,O chelated Ni(II) complexes were studied for ethylene polymerization in aqueous emulsion. Complexes based on enolatoimine ligands bearing electron-withdrawing trifluoromethyl and trifluoroacetyl groups [κ^2-*N*,*O*-{2,6-$R_2C_6H_3N$═C(H)C($COCF_3$)═C(O)CF_3}]Ni(L)Me (**4a**, R = ^{i}Pr, L = pyridine; **4b**, R = 3,5-$(CF_3)_2C_6H_3$, L = pyridine; **5b**, R = 3,5-$(CF_3)_2C_6H_3$, L = PPh_3) were prepared. The complexes are very active in aqueous emulsions, with 1.4×10^4 TO h^{-1} for **4a** (50 °C) and 1.9×10^4 TO h^{-1} for **4b** (70 °C), affording stable polyethylene dispersions. The phosphine complex **5b** is active in the absence of a phosphine scavenger, with similar activities as **4b**. Polyethylenes of typically M_w 3×10^4 g mol^{-1} (M_w/M_n 2.0−2.5) with 25−50 branches per 1000 carbon atoms and T_m 94−112 °C are obtained.

Introduction

Polymer dispersions are produced industrially on a large scale by emulsion polymerization. They are employed increasingly for a variety of environmentally benign applications, such as coatings and paints.[1] Emulsion polymerization is carried out in a free radical fashion industrially. By contrast to radical polymerization, catalytic polymerization allows for a control of microstructure, and correspondingly material properties, over a wide range. In terms of the polymerizable monomers, both types of polymerization are largely complementary.

The synthesis of polyethylene dispersions by catalytic polymerization has been studied recently.[2−4] By polymerization of ethylene with Ni(II) salicylaldiminato complexes, high molecular weight polyethylene dispersions can be prepared.[2b,c,f,h,j] By appropriately tailoring the catalyst via remote substituents of *N*-terphenyl moieties in the salicylaldimine backbone linear, semicrystalline or highly branched, amorphous polymer can be prepared. The latter goes at the expense of molecular weight, however.[2f]

Catalyst activity is an issue in polymerization with neutral Ni(II) complexes in general and in aqueous systems in particular. An increased electrophilicity of the Ni center, brought about by electron-withdrawing substituents in the bidentate N, O- or P, O-coordinating ligand, substantially increases the polymerization rates.[5,6] Recently, Brookhart et al. reported that enolatoimine Ni(II) phenyl complexes [κ^2-*N*,*O*-{ArN═CH−C($COCF_3$)═C(CF_3)O}NiPh(L)] (Ar = 2,6-$^iPr_2C_6H_3$) are very active for ethylene polymerization, activities exceeding those of all previously reported neutral κ^2-N,O Ni(II) complexes.[7] By contrast to electron-poor phosphinoenolate complexes, which have also been studied for the synthesis of low molecular weight polyethylene dispersions (M_n ca. 2×10^3 g mol^{-1}),[3b] these κ^2-N,O Ni(II) complexes afforded higher molecuar weight polymer. This makes them interesting candidates for the synthesis of polymer dispersions by polymerization in aqueous systems. However, with increasing electrophilicity of the metal center, an increased reactivity and sensitivity toward water must also be anticipated.[8]

Scheme 1. Synthesis of Ketoenamines 3a−c

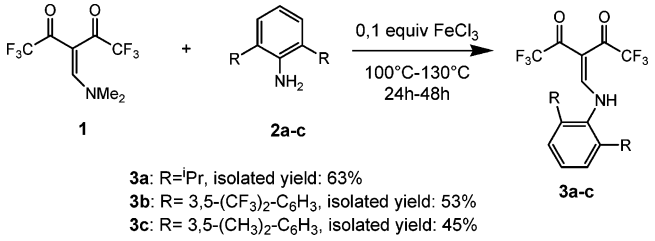

We now report on the behavior of Ni(II) catalysts with electron-poor enolatoimine ligands in aqueous systems. Several novel Ni(II) complexes were prepared for this purpose. Crystallinity of the polyethylene formed, and its control via the catalyst, are also of strong interest in view of film formation from dispersions. For this reason, ligands and complexes with *N*-aryl groups differing in steric bulk and electronic properties were studied.

Results and Discussion

Synthesis and Characterization of Ketoenamine Ligands. The novel ketoenamines **3b,c** and the previously described **3a** were prepared by reaction of *N*,*N*-dimethylaminomethylene-1,1,1,5,5,5-hexafluoroacetylacetone (DMAMFA, **1**)[9] with the corresponding 2,6-disubstituted anilines (**2**)[2f,10] in a modified literature procedure. Prolonged reaction of **1** with the anilines (24 h for **2a**, 48 h for **2b,c**) in the presence of 0.1 equiv of anhydrous $FeCl_3$ in the bulk at elevated temperature afforded **3a**−**c**. The crude products were purified by column chromatography. The ketoenamines were obtained in satisfactory yields (Scheme 1).

The identity and purity of compounds **3a**−**c** were unambiguously established by ^{1}H and ^{13}C NMR, elemental analysis, and mass spectroscopy. NMR assignements were confirmed by ^{1}H, ^{1}H gCOSY, ^{1}H, ^{13}C gHMQC, ^{1}H, ^{13}C gHMBC, and DEPT. Spectroscopic data for **3a** are in agreement with the data reported recently by Brookhart (in $CDCl_3$ vs C_6D_6 used in this work).[7]

* Corresponding author: e-mail stefan.mecking@uni-konstanz.de.

10.1021/ma061804n CCC: $37.00
Published on Web 01/11/2007

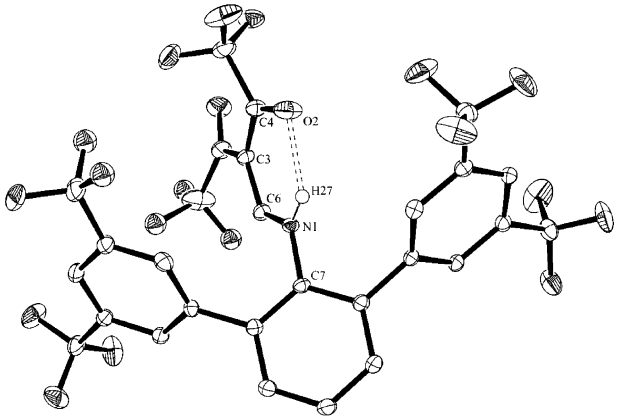

Figure 1. X-ray crystal structure of **3b**.

In C_6D_6 solution, all compounds exist exclusively as the ketoenamine tautomer. The N*H* proton resonates at 11.4−12.2 ppm in **3a**−**c**. ^3J-coupling to the HN−C*H*═ proton can be observed (12−14 Hz). This low-field shift suggests that the favored geometries are U-shaped to accommodate H-bonding between N−H and the carbonyl oxygen, as suggested by Brookhart for **3a**. Also, two separate, but similar, shifts are observed for the C═O and CF_3 groups in ^{13}C and ^{19}F spectra, respectively. This indicates that both carbonyl groups are in the keto form.

The solid-state structure of **3b** was determined by single-crystal X-ray diffraction (Figure 1). Suitable crystals of **3b** were grown from methylene chloride/pentane at −30 °C. Crystallographic data and experimental details of the data collection and structure refinement are given in the Experimenal Section and the Supporting Information. The fluorine atoms of the trifluoromethyl substituents were found to be disordered, which is not an uncommon behavior for such groups. The disorder was refined by the splitting of the atom occupancy factors of the corresponding fluorine atoms. Therefore, the latter are refined using isotropic displacement factors.

Like in solution, **3b** exists as the ketoenamine also in the solid. This is evident from bond length; also, the NH proton could be resolved (Figure 1). The atoms O2−C4−C3−C6−N1−H27 establish a planar six-membered H-chelate. The maximum deviation from the least root-mean-square (rms) plane defined by all six atoms is only 0.064 Å. By comparison, the corresponding deviations from the least rms plane of the phenyl entities ranges between 0.010 and 0.003 Å. C−O double bond distances are found to fit in the typical range (1.23 Å) for electron-deficient carbonyl entities. The bond lengths C3−C2 and C3−C4 (1.45−1.46 Å) correspond to C−C single bonds adjacent to strongly electron-withdrawing groups, in this case the C(O)CF_3 entities. The bond distance between atoms C3−C6 is 1.393(3) Å and resembles typical partial double bond character as in aromatic rings (1.395(3) Å).[11] The N−C6 bond length of 1.326(3) Å is in accordance with a single bond adjacent to a conjugated system.[11] The distance H27−O2 was estimated to 1.9 Å. The aforementioned plane of the H-bridged ketoenamine system (O2−C4−C3−C6−N1−H27) and the central phenyl ring of the terphenylamine entity incline at an angle of 51.7(3)°. The two 3,5-bis(CF_3)-substituted phenyl rings and the central phenyl ring incline at angles of 63° and 53°, respectively. The corresponding angles of inclination to the H-bridged ketoenamine system are 87° and 42°, respectively.

Synthesis and Characterization of Complexes. [(tmeda)-Ni(CH_3)$_2$][12] was employed as a Ni(II) source (tmeda = *N*,*N*,*N*′,*N*′-tetramethylethylenediamine). Reaction with the ketoenamines results in expulsion of one Ni−Me group as methane to afford the square-planar complexes **4a,b** (Scheme 2). The new compounds were characterized by ^1H, ^{13}C, and ^{19}F NMR spectroscopy as well as elemental analysis. The ^{13}C NMR resonances were fully assigned by ^1H, ^1H gCOSY, heteronuclear ^1H, ^{13}C 2D NMR and ^1H, ^{13}C 2D long-range-coupling NMR spectroscopy. For **4a**, the septet due to the CH protons of the isopropyl groups is shifted downfield vs the free ligand **3a** (2.68 ppm) to 3.98 ppm in **4a**. Coordination to the metal center results in splitting of the methyl resonances of the isopropyl groups into two doublets, as the methyl groups of a given isopropyl moiety experience different environments (1.12 and 1.45 ppm vs 0.89 ppm in the free ligand). Rotation around the aryl−isopropyl bond and around the *N*-aryl bond is hindered. The characteristic NH signal (11.94 ppm) of the ketoenamine has completely disappeared. Instead of the doublet observed in the free ligand (7.80 ppm), the N−CH═ proton is observed as a singlet at 8.02 ppm in the complex. Overall, the signals originating from the enolatoimine ligand (N^O) in **4a** are similar to the signals reported previously[7] for the related compound [(N^O)NiPh(PPh_3)].

For the CF_3-substituted aryl rings, only one signal is observed for the CF_3 groups and the o- and m-carbon atoms, respectively, in the ^{13}C NMR spectra. In accordance, also only one signal is observed for the CF_3 group in the ^{19}F NMR spectrum. This indicates a rapid rotation of the CF_3-substituted aryl rings along the bond to the central N-bound aryl ring, contrasting the hindered rotation observed in the ^{i}Pr-substituted complex **4a**.

For both complexes, only a single Ni−Me resonance is observed. This shows that only one isomer with respect to the stereochemistry at the square-planar Ni(II) center is formed. By analogy to similar compounds, for which the solid-state structure was determined by single-crystal X-ray diffraction, it can be assumed that the Ni-bound Me group is trans to the oxygen donor.[2f,13]

Somewhat suprisingly, the analogous reaction of ketoenamine **3c** with [(tmeda)Ni(CH_3)$_2$] under the same reaction conditions did not afford the desired analogue of **4a,b**. Apparently, the xylyl-substituted ketoenamine **3c** has a different reactivity by comparison to the 3,5-bis(trifluoromethyl)phenyl-substituted

Scheme 2

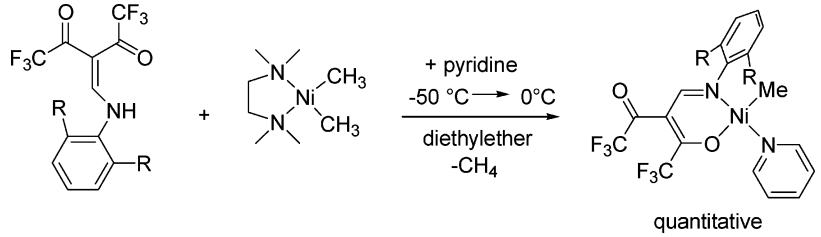

quantitative

4a: R= ^{i}Pr
4b: R= 3,5-$(CF_3)_2$-C_6H_3

Scheme 3

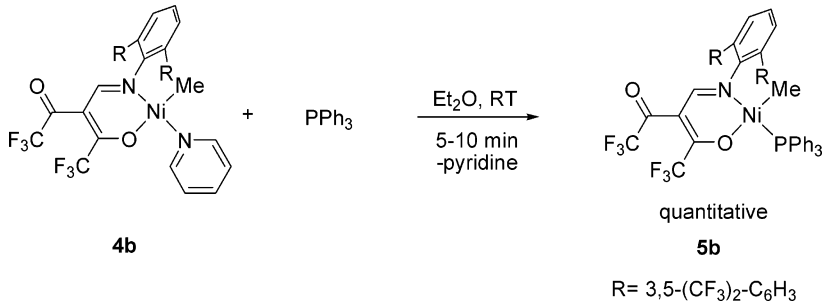

4b **5b**

R= 3,5-$(CF_3)_2$-C_6H_3

Table 1. Polymerization under Nonaqueous Conditions[a]

entry	catalyst precursor	cat. [10^{-6} mol]	*p*(ethylene) [bar]	temp [°C]	*t* [h]	TOF [mol(C_2H_4) mol (Ni)$^{-1}$·h^{-1}]	polymer yield [g]	M_w[b] [g mol^{-1}]	M_w/M_n	crystallinity[c] [%]	T_m [°C]
1-1	[(tmeda)$NiMe_2$]/**3a**	40	15	30−75	0.25	54 700	15.3	28 000	3.6	28	96
1-2	[(tmeda)$NiMe_2$]/**3a**	20	40	30	0.67	26 500	9.9	30 000	3.4	33	97
1-3	[(tmeda)$NiMe_2$]/**3a**	20	20	45	1	9 800	5.5	36 000	2.2	35	99
1-4	[(tmeda)$NiMe_2$]/**3a**	20	20	40	0.5	10 000	2.8	43 000	2.4	37	98
1-5	[(tmeda)$NiMe_2$]/**3a**	20	20	50	0.5	46 800	13.1	32 000	2.3	32	98
1-6	[(tmeda)$NiMe_2$]/**3a**	20	20	60	0.5	21 800	6.1	25 000	2.6	32	99
1-7	[(tmeda)$NiMe_2$]/**3a**	20	20	70	0.5	19 600	5.5	16 000	2.6	29	94
1-8	**4a**	20	20	50	0.5	9 100	2.6	29 000	2.9	34	96
1-9	**4a**	20	40	60	0.25	138 000	19.3	24 000	3.0	35	97
1-10	**4a**	20	40	70	0.25	52 100	7.3	19 000	2.4	29	95
1-11	[(tmeda)$NiMe_2$]/**3b**	10	20	50	1	1 100	0.3	37 000	2.4	35	111
1-12	[(tmeda)$NiMe_2$]/**3b**	10	30	50	1	1 800	0.5	40 000	2.3	36	110
1-13	[(tmeda)$NiMe_2$]/**3b**	20	40	60	1	1 100	0.6	30 000	2.5	45	110
1-14	**4b**	20	10	60	0.5	14 200	4.0	29 000	2.4	45	108
1-15	**4b**	20	20	60	0.5	27 500	7.7	35 000	2.3	48	109
1-16	**4b**	20	40	60	0.5	30 900	9.7	36 000	2.3	45	110
1-17	**4b**	20	40	50	0.5	23 600	6.6	54 000	2.6	36	112
1-18	**4b**	20	40	70	0.5	78 200	21.9	28 000	2.4	40	108
1-19	**4b**	20	40	80	0.5	81 100	22.7	23 000	2.3	39	106
1-20	**4b**	10	40	60	4	24 600	27.5	38 000	2.3	40	110
1-21	**5b**	10	40	70	1	81 400	22.8	32 000	2.1	44	109
1-22	**5b**/[$Ni(cod)_2$][d]	5	40	70−100	1	167 100	23.4	21 000	5.1	35	106

[a] Reaction conditions: 100 mL of toluene. [b] Determined by GPC vs linear polyethylene standards. [c] Determined by DSC. [d] 2 equiv of [$Ni(cod)_2$] added as a phosphine scavenger (PPh_3/[$Ni(cod)_2$] molar ratio 1:2).

analogue **3b**, despite the remoteness of the differing substituents from the reacting groups. The reason for this different reactivity is not apparent. A higher reactivity of **3b** due to a higher acidity of the NH moiety resulting from the electron-withdrawing CF_3-aryl groups would be a possible explanation; however, this appears inconclusive with the observed behavior of the isopropyl-substituted **3a** which should be even more electron rich than **3c**.

The triphenylphosphine complex **5b** was prepared conveniently by pyridine displacement from **4b** (Scheme 3). ^{31}P NMR spectra at ambient temperature of a solution of equimolar amounts of **4b** and PPh_3 in C_6D_6 display two signals at −3.9 ppm (free PPh_3) and at 31.6 ppm (coordinated phosphine). This indicates a competition of pyridine and PPh_3 for binding at nickel. By evaporating of the solvent and drying in vacuo, the phosphine complex **5b** was obtained cleanly. The equilibrium is shifted toward the PPh_3 complex due to the volatility of pyridine. The compound was characterized by ^1H, ^{13}C, and ^{31}P NMR and elemental analysis. In the ^1H NMR spectrum of **5b**, the Ni−Me resonance appears at −1.07 ppm vs −0.73 ppm in **4b**. A P−H coupling is not observed for this signal; however, the methyl signal is relatively broad. This can be an indication of coupling with a low coupling constant (estimated 4 Hz or less). Coordination of PPh_3 seems unambiguous, however, in view of the ^{31}P shift observed. In ^{13}C NMR spectra, a coupling between the phosphorus atom of PPh_3 and the carbon atom of the methyl group bound to the nickel center is observed, as expected. The imine proton *H*C═N resonates at 7.73 ppm vs 7.48 ppm in the pyridine analogue **4b**.

Polymerization Studies in Nonaqueous System. In addition to polymerization in aqueous emulsions, polymerizations in toluene were also studied. By contrast to the aqueous multiphase system, the nonaqueous system at least initially consists of only a single phase, in which catalyst concentration and monomer concentration are known. Also, such comparative reactions yield insights on the water sensitivity of the catalyst.

In addition to studies of the aforementioned complexes **4a,b** and **5b** as catalyst precursors, catalysts prepared in situ by reaction of [(tmeda)$Ni(CH_3)_2$] with ketoenamines **3a,b** were studied (Table 1).

For [(tmeda)$Ni(CH_3)_2$]/**3a**, with 40 μmol of catalyst the exothermic reaction could not be controlled under the conditions studied (100 mL of toluene, 15 atm). The reaction temperature rose above 75 °C (entry 1-1). At half the catalyst amount, the reaction temperature could be controlled. Activities on the order of 10^4−10^5 TO h^{-1} were observed. These activities are comparable with known neutral κ^2-*N*,*O*-salicylaldiminato Ni(II) complexes.[2f,5] In some experiments, the reaction was monitored by measuring the ethylene flow with mass flow meters. Albeit activity decreases with time, residual activity (entry 1-4: 4 g h^{-1} = 7.1 × 10^3 TO h^{-1}; entries 1-3, 1-5, and 1-7: ca. 1.5 g h^{-1} = 2.7 × 10^3 TO h^{-1}) was still observed at the end of the polymerization run which lasted 30 min (entry 3: 60 min). A study of the influence of reaction temperature showed that the catalyst obtained from [(tmeda)$Ni(CH_3)_2$]/**3a** is most productive at 50 °C (entries 1-4 to 1-7). Polymer molecular weights decrease with increasing temperature, as expected. With increasing temperature, the rate of chain transfer increases relative to

the chain growth rate. With complex **4a** as a catalyst precursor, activity is lower vs [(tmeda)Ni(CH_3)$_2$]/**3a** at 50 °C, which is the optimum temperature for the latter system. At 60 °C, which was found to be the optimum temperature for **4a** (entries 1-8 to 1-10), the activity observed for **4a** exceeds that of the in-situ system. At the end of this 15 min polymerization experiment, a strong consumption of ethylene (ca. 31 g h^{-1} = 5.5 × 10^4 TO h^{-1}) was still detected. The pyridine complex requires higher polymerization temperatures to enhance pyridine dissociation, pyridine binding stronger to the Ni(II) center by comparison to the tertiary amine tmeda present in the in-situ system. However, the pyridine complex affords a catalyst which is more stable at elevated temperature, possibly due to stabilization by intermittent pyridine coordination. A similar behavior has been observed for salicylaldimine-substituted catalysts.[14] A difference in detail is that for in-situ systems [(tmeda)NiMe_2]/ligand; for salicylaldimines a high activity was observed already at polymerization temperatures of 20 °C, but rapid decomposition was observed at ≥30 °C, whereas for the ketoenamines studied in this work 50 °C was required for efficient polymerization. This may be due to a stronger coordination of tmeda due to the electron deficiency of the Ni(II) center, which results from the strongly electron-withdrawing enolatoimine ligand.

Studies of the CF_3-aryl substituted ligand **3b** as an in-situ catalyst system [(tmeda)NiMe_2]/**3b** revealed only moderate activities (entries 1-11 to 1-13). By contrast, high activities are observed with the pyridine complex (**4b**) as a catalyst precursor (entries 1-14 to 1-20). Likely, undesired side reactions occur in the reaction of **3b** with [(tmeda)NiMe_2] in the absence of pyridine. With the pyridine complexes as catalyst precursors, high activities are observed even at a polymerization temperature of 80 °C. The catalyst is remarkably temperature stable. In a polymerization experiment carried out at 60 °C with a prolonged reaction time of 4 h, an almost linear increase in polymer yield with time is observed vs a shorter experiment (entry 1-20 vs 1-16), evidencing a high stability over time at this temperature. A study of the effect of ethylene pressure (that is, monomer concentration) revealed that from 10 to 20 atm activity increases almost linearly, but the effect of pressure on activity levels off at higher pressures. This is indicative of competitive binding of pyridine vs monomer to the metal center, which plays a lesser role at high ethylene concentrations; that is, saturation of the binding equilibrium occurs at ethylene pressures higher than ca. 20 bar.

Preliminary studies were carried out with the phosphine complex **5b**. The phosphine was expected to bind relatively strongly to the metal center. For a phosphine complex based on ligand **3a**, [κ^2-*N*,*O*-{ArN=CH−C($COCF_3$)=C(CF_3)O}NiPh(PPh_3)] (Ar = 2,6-$^i Pr_2C_6H_3$), Brookhart found a moderate activity, which was very much enhanced only in the presence of a phosphine scavenger. Surprisingly, **5b** exhibits a rather high activity without any scavenger (entry 1-21). The activity observed in this experiment is similar to the pyridine complex **4b** under analogous conditions (70 °C). After a polymerization time of 1 h, a significant ethylene consumption (10 g h^{-1} = 3.5 × 10^4 TO h^{-1}) was still detected. Activation of **5b** by [Ni(cod)$_2$] (cod = 1,5-cyclooctadiene) as a phosphine scavenger[15] was studied (entry 1-22). A rapid ethylene uptake occurred, and the reaction temperature rose from 70 to >100 °C. At the end of this 1 h polymerization experiment, a strong ethylene consumption was still observed (10 g h^{-1} = 7 × 10^4 TO h^{-1}). This indicates that the catalyst is stable even at these high temperatures. As a consequence of the failure of temperature control, the molecular weight distribution of the resultant polymer is relatively broad (M_w/M_n 5.1).

Overall, the polymerization experiments show that displacement of the ligand L from [(N^O)NiR(L)] (R = alkyl: Me or growing polymer chain; L = tmeda, pyridine, PPh_3) to form active species [(N^O)NiR(ethylene)] is a critical step, which likely limits activities.

The polymer molecular weights and melting points obtained with a given ketoenamine ligand (**3a** or **3b**) at a given polymerization temperature are independent of the type of catalyst system used (pyridine complex, in-situ system [(tmeda)Ni(CH_3)$_2$]/ketoenamine, or phosphine complex **5b**). This confirms that the active species formed from the different catalyst precursors are identical for a given ketoenamine ligand, as anticipated. Molecular weight distributions M_w/M_n close to 2 indicate a well-behaved single site nature of the active species.

The microstructure of the polymers was studied by quantitative ^{13}C NMR. The major branches are methyl branches. In addition, ethyl and higher branches are observed. For example, the polymer from entry 1-7 (ketoenamine ligand **3a**) has ca. 35 Me branches, 7 Et branches, and 10 C_{4+} branches per 1000 carbon atoms. By comparison, the polyethylene from entry 1-18 (catalyst precursor **4b**) has ca. 20 Me branches, 1 Et branch, and 4 C_{4+} branches per 1000 carbon atoms. The overall branching observed for polymers prepared with catalysts based on the isopropyl-substituted ketoenamine **3a** is higher than for the CF_3-aryl substituted ketoenamine **3b**, ca. 50 branches vs ca. 25 branches (entry 1-7 vs 1-18). This results in a higher crystallinity and melting point for the polymers prepared with the latter catalysts (Table 1).

Polymer molecular weights are on the order of M_n 10^4 g mol^{-1} in all cases. In detail, somewhat higher molecular weights are observed with catalysts based on **3b** vs **3a** under otherwise identical reaction conditions. As expected, the molecular weights and molecular weight distributions observed with catalysts based on ketoenamine **3a** (entries 1-1 to 1-10) agree well with data reported by Brookhart et al. for polymers prepared with the complex [κ^2-*N*,*O*-{ArN=CH−C($COCF_3$)=C(CF_3)O}NiPh(PPh_3)] (Ar = 2,6-$^i Pr_2C_6H_3$) of the same ketoenamine as a catalyst precursor (activated with a phosphine scavenger).[7]

Synthesis of Aqueous Dispersions. To prepare a polymer dispersion, a high degree of dispersion of the catalyst precursor in the initial reaction mixture is required. For a lipophilic catalyst precursor, this can be achieved by a miniemulsion technique.[2c,3b,16] Pyridine complexes were dissolved in a small amount of toluene (2 mL). The solution was miniemulsified in an aqueous SDS solution by means of high shear generated by ultrasonication. Exposure to ethylene in a pressure reactor afforded stable dispersions (Table 2). This demonstrates that despite the strongly electron-withdrawing nature of the enolatoimine ligands in the catalysts studied, catalyst stability toward water is sufficient to carry out polymerization in aqueous systems. An average catalyst activity of 1.9 × 10^4 TO h^{-1} was observed with **4b** at 70 °C (entry 2-8). At the end of this 1 h polymerization experiment an ethylene consumption corresponding to a residual activity of 1.6 × 10^4 TO h^{-1} was observed. The catalyst activities observed rival the highest activities reported to date for the synthesis of polyethylene dispersion with salicylaldiminato complexes. A preliminary study of the phosphine complex **5b** in aqueous emulsion with [Ni(cod)$_2$] as a phosphine scavenger shows that this catalyst precursor is also suited for polymerization in aqueous systems (entry 2-10). This is not necessarily to be expected from the aforementioned studies (entries 1-21, 1-22, and 2-6 to 2-9) as the high local concentration of the reagents, particularly lipophilic phosphine, in the

Table 2. Polymerization in Aqueous Emulsion.[a]

entry	cat.	temp [°C]	solids content[b] [%]	TOF [mol (C_2H_4) mol (Ni)$^{-1}$·h^{-1}]	M_w[c] (g·mol^{-1})	M_w/M_n	crystallinity[d] [%]	T_m [°C]	particle size[e] [nm]
2-1	**4a**	40	2.4	4600	38 000	2.1	36	100	180
2-2	**4a**	50	7.0	13 600	41 000	2.6	38	101	157
2-3	**4a**	60	5.7	10 800	34 000	2.3	39	100	155
2-4	**4a**	70	1.0	2 000	n.d.	n.d.	n.d.	n.d.	128
2-5	**4a**	50	10.0	10 000	40 000	2.4	39	99	127
2-6	**4b**	50	1.3	2 500	51 000	2.0	42	111	91
2-7	**4b**	60	5.0	9 800	40 000	2.2	37	110	139
2-8	**4b**	70	9.0	18 500	36 000	2.5	40	108	544
2-9	**4b**	80	7.0	14 200	27 000	2.1	38	106	454
2-10[f]	**5b**	70	2.5	9 500	24 000	2.9	44	110	225

[a] Reaction conditions: 98 mL of water, 0.75 g of SDS, 0.1 mL of hexadecane, 2 mL of toluene; 20 μmol of catalyst precursor (entry 2-10: 10 μmol); ethylene pressure: 40 bar; reaction time: 1 h (entry 2-5: 2 h). [b] Polymer solids content: no coagulate observed. [c] Determined by GPC vs linear polyethylene standards. [d] Determined by DSC. [e] Volume average particle size determined by DLS. [f] 2 equiv of [Ni(cod)$_2$] added as a phosphine scavenger. n.d. = not determined.

Table 3. Details of the Crystal Structure Determination of 3b

formula	$C_{28}H_{11}F_{18}NO_2$
fw	735.38
cryst size, mm	0.5 × 0.4 × 0.4
space group	*P*21
a, Å	8.2269(5)
b, Å	15.4634(10)
c, Å	11.0881(7)
α, deg	90
β, deg	99.872(5)
γ, deg	90
V, Å^3	1389.70(15)
Z	2
δ_{calc}, g cm^{-3}	1.757
T, K	100
μ, mm^{-1}	0.193
F(000)	728
Θ_{max}, deg	29.25
no. of rflns measd	26378
no. of unique rflns	7480
no. of rflns $I > 2\sigma(I)$	6766
R_1, $I > 2\sigma(I)$[a]	0.0476
R_1, all data	0.0528
wR_2[a]	0.1191
diff Fourier peak min/max, e Å^{-3}	−0.46/0.50

[a] $R_1 = \sum||F_o| - |F_c||/\sum|F_o|$, $wR_2 = [\sum w(F_o^2 - F_c^2)^2)/\sum w(F_o^2)^2)]^{1/2}$.

aqueous system by comparison to nonaqueous polymerizations can affected catalyst activation and activity.

By comparison to polymerizations in nonaqueous systems (Table 1), activity is reduced 5−10-fold. A similar behavior has been found for catalysts based on other types of neutral Ni(II) complexes.[2c,f,3b] A possible explanation is deactivation of a part of the catalyst precursor upon preparation of the miniemulsion or in the early stages of the polymerization experiment.

Dispersions of up to 10 wt % polymer solids content were obtained, without further optimization. Volume average particle sizes are in the range of 100−600 nm. Polymer molecular weights and molecular weight distributions and crystallinities determined on bulk samples are similar to the properties found for polyethylenes prepared in nonaqueous systems (Tables 1 and 2). This also applies to overall degrees of branching and branch types. TEM micrographs (Figure 2) show the particles to be spherical. Some film formation appears to occur on the boundaries of the particles. (From studies of comparative samples, it can be excluded that this is an artifact caused by surfactant.) These observations contrast to previous studies on latex particles of more crystalline, linear polyethylene, which are lentil-shaped due to lamella stacking and do not coalesce at their boundaries due to the high crystallinity.[2e]

Summary and Conclusions. Neutral Ni(II) complexes based on enolatoimine ligands with strongly electron-withdrawing trifluoromethyl and trifluoroacetyl groups were studied as catalyst precursors for ethylene polymerization. Despite the electron-deficient nature of the metal centers, which can enhance deactivation reactions such as hydrolysis or coordination of water, polymerizations can be carried out in aqueous systems to afford polyethylene dispersions. Even at high temperatures of 70 °C catalyst stability is sufficient for the polymerization to continue for hours. Catalyst activities of up to 1.9 × 10^4 TO h^{-1} (70 °C polymerization temperature) were observed in aqueous systems. This rivals the highest activties reported for neutral Ni(II) salicylaldiminato complexes, which were the only complexes reported to date to afford polyethylene dispersions of higher molecular weight material ($M_n \geq 10^4$ g mol^{-1}).[14]

Studies of different catalyst precursors, [(N^O)NiMe(L)] with L = pyridine or PPh_3, or in situ prepared catalysts [(tmeda)-$NiMe_2$]/ketoenamine, show that exchange of the coordinating ligand L is a critical step for the electron-poor Ni(II) complexes studied and likely is one limiting factor for catalyst activities.

The substitution pattern of the N-bound aryl group (N−$C_6H_3R_2$) influences the degree of branching of the polymer formed and correspondingly its crystallinity and melt temper-

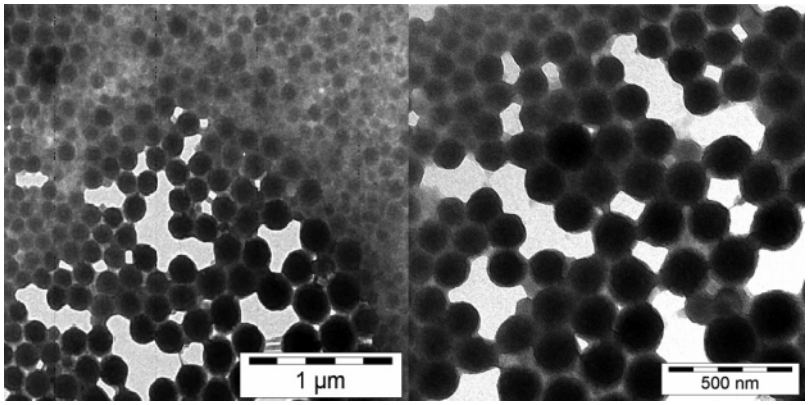

Figure 2. TEM images of polymer particles (Table 2, entry 2-2).

ature. For R = isopropyl a total degree of branching of 40−50 is observed (crystallinity ≈ 35%, T_m ≈ 97 °C) vs ca. 25 branches/1000 carbon atoms (crystallinity ≈ 45%, T_m ≈ 110 °C) for R = 3,5-$(F_3C)_2C_6H_3$.

Experimental Section

Materials and General Considerations. Unless noted otherwise, all manipulations of nickel complexes were carried out under an inert atmosphere using standard glovebox or Schlenk techniques. All glassware was flame-dried under vacuum before use. Toluene and pentane were distilled from sodium, and diethyl ether from sodium/benzophenone under argon. Hexadecane was degassed under argon. Demineralized water was distilled under nitrogen and degassed three times after distillation. Pyridine was distilled from CaH_2. [(tmeda)$NiMe_2$] was supplied by MCAT (Konstanz, Germany). 1,1,1,5,5,5-Hexafluoro-2,4-pentanedione (99% purity) and 2,6-diisopropylaniline (90% purity, technical) were obtained from Acros. Substituted terphenylanilines (**2b,c**) were prepared according to published procedures.[2f]

NMR spectra were recorded on a Varian Unity INOVA 400 or on a Bruker AC 250 spectrometer. ^{1}H and ^{13}C NMR chemical shifts were referred to the solvent signal. High-temperature NMR measurements of polyethylenes were performed in 1,1,2,2-tetrachloroethane-d_2 at 130 °C. The branching structure was assigned according to ref 17. Differential scanning calorimetry (DSC) was performed on a Netzsch Phoenix 204 F1 at a heating and cooling rate of 10 K min^{-1}. DSC data reported are from second heating cycles. Polymer crystallinities were calculated on the basis of a melt enthalpy of 293 J g^{-1} for 100% crystalline polyethylene. Gel permeation chromatography (GPC) was carried out in 1,2,4-trichlorobenzene at 160 °C on a Polymer Laboratories 220 instrument equipped with Mixed Bed PL columns. Data reported were referenced to linear polyethylene standards. Dynamic light scattering was carried out on a Malvern Nano Zeta Sizer. For the determination of particle size, a few drops of a latex sample were diluted with ca. 3 mL of water. The TEM images were obtained by Dr. Ralf Thomann at the University of Freiburg on a LEO 912 instrument. The acceleration voltage was 120 keV, and the samples were not contrasted. Elemental analyses were performed up to 950 °C on an Elementar Vario EL.

Synthesis of *N,N*-Dimethylaminomethylene-1,1,1,5,5,5-hexafluoroacetylacetone (DMAMFA, 1) was carried out according to a published procedure.[9] In brief, in a 50 mL flask equipped with a reflux condenser with a drying tube and magnetic stirr bar, a mixture of 1,1,1,5,5,5-hexafluoro-2,4-pentanedione (5 g, 24 mmol), dimethylformamide (1.75 g, 24 mmol), and acetic acid anhydride (24 mL) was heated to 80 °C for 8 h. Ac_2O and the AcOH formed were removed by distillation. The residue was distilled under vacuum (80 °C/4mbar) to afford **1** in 83% yield. ^{1}H NMR (250 MHz, $CDCl_3$, 25 °C): δ/ppm = 7.71 (s, 1H, C═C*H*), 3.43 (s, 3H, CH_3), 2.80 (s, 3H, CH_3). ^{13}C NMR (400 MHz, $CDCl_3$, 25 °C): δ/ppm = 179.2 (q, $^2J_{CF}$ = 36 Hz, CF_3CO), 157.8 (s, *C*H═C), 115.3 (q, $^1J_{CF}$ = 292.5 Hz, CF_3), 101.0 (s, *C*═CH), 48.5 (s, *C*H_3), 45.3 (s, *C*H_3).

Synthesis of the Ketoenamines (3a−c). Equimolar amounts of *N,N*-dimethylaminomethylene-1,1,1,5,5,5-hexafluoroacetylacetone (**1**) and aniline (**2a**−**c**) were stirred at elevated temperature (100−130 °C) in the presence of 0.1 equiv of $FeCl_3$ under argon (reaction time **3a**: 24 h; **3b**,**c**: 48 h). The crude compound was purified by column chromatography (**3a**: petrolether/CH_2Cl_2 1:1, yield: 63%. **3b**: petrolether/Et_2O 3:1, yield: 53%. **3c**: toluene/CH_2Cl_2 5:1, gradient chromatography, yield: 45%).

3-[{(2,6-Diisopropylphenyl)amino}methylene]-1,1,1,5,5,5-hexafluoropentane-2,4-dione (3a). ^{1}H NMR (400 MHz, C_6D_6, 25 °C): δ/ppm = 11.94 (d, $^3J_{HH}$ = 14 Hz, 1H, N*H*), 7.80 (d, $^3J_{HH}$ = 14 Hz, 1H, vinylic *H*C═C), 7.00 (t, $^3J_{HH}$ = 7.6 Hz, 1H, C*H* para to NH), 6.84 (d, $^3J_{HH}$ = 7.6 Hz, 2H, C*H* meta to NH), 2.68 (sept, $^3J_{HH}$ = 6.8 Hz, 2H, ^{i}Pr C*H*), 0.89 (d, $^3J_{HH}$ = 6.8 Hz, 12H, ^{i}Pr CH_3). ^{13}C NMR (100 MHz, C_6D_6, 25 °C): δ/ppm = 181.74 (q, $^2J_{CF}$ = 39 Hz, CF_3CO), 175.15 (q, $^2J_{CF}$ = 34 Hz, CF_3CO), 162.31 (vinylic *C*H═C), 143.80 (ortho *C*), 133.89 (ipso *C*), 129.92 (para *C*), 124.57 (meta *C*), 117.38 (q, $^1J_{CF}$ = 291 Hz, *C*F_3), 117.28 (q, $^1J_{CF}$ = 286 Hz, *C*F_3), 102.02 (vinylic *C*═CH), 28.71 (^{i}Pr *C*H) and 23.36 (^{i}Pr *C*H_3). ^{19}F NMR (375 MHz, C_6D_6, 25 °C): δ/ppm = −73.76 and −70.74 (CF_3CO). Anal. calcd (%) for $C_{18}H_{19}F_6NO_2$: C, 54.69; H, 4.84; N, 3.54. Found: C, 55.05; H, 5.03; N, 3.57. MS (*m*/*z*, %): 395 (55.4, M^+).

3-[{(2,6-Di(3,5-bis(trifluormethyl)phenyl)phenyl)amino}methylene]-1,1,1,5,5,5-hexafluoropentane-2,4-dione (3b). ^{1}H NMR (400 MHz, C_6D_6, 25 °C): δ/ppm = 11.44 (d, $^3J_{HH}$ = 13 Hz, 1H, N*H*), 7.72 (s, 2H, para *H* of the CF_3 substituted aryl rings), 7.37 (s, 4H, ortho C*H* of the CF_3 substituted aryl rings), 6.88 (t, $^3J_{HH}$ = 8 Hz, 1H, C*H* para to NH), 6.83 (d, $^3J_{HH}$ = 13 Hz, 1H, vinylic *H*C═C), 6.66 (d, $^3J_{HH}$ = 8 Hz, 2H, C*H* meta to NH). ^{13}C NMR (100 MHz, C_6D_6, 25 °C): δ/ppm = 181.96 (q, $^2J_{CF}$ = 38.3 Hz, CF_3CO,), 175.13 (q, $^2J_{CF}$ = 34.7 Hz, CF_3CO,), 159.73 (q, $^4J_{CF}$ = 4 Hz, vinylic *C*H═C), 138.53 (ipso *C* of the CF_3 substituted aryl rings), 134.22 (s, *C* ortho to NH), 133.21 (*C* ipso to NH), 133.02 (q, $^2J_{CF}$ = 34.7 Hz, *C*CF_3), 131.77 (*C* meta to NH), 129.60 (ortho *C* of the CF_3 substituted aryl rings), 129.29 (*C* para to NH), 123.32 (q, $^1J_{CF}$ = 271.7 Hz, *C*F_3 of the aryl rings), 122.52 (para *C* of the CF_3 substituted aryl rings), 116.52 (q, $^1J_{CF}$ = 286 Hz, *C*F_3CO), 116.42 (q, $^1J_{CF}$ = 291 Hz, *C*F_3CO), 115.09 (vinylic *C*═CH). ^{19}F NMR (376 MHz, C_6D_6, 25 °C): δ/ppm = −63.41 (aryl CF_3), −72.45 and −74.41 (CF_3CO). Anal. calcd (%) for $C_{28}H_{11}F_{18}NO_2$: C, 45.73; H, 1.51; N, 1.90. Found: C, 45.85; H, 1.84; N, 2.02. MS (*m*/*z*, %): 735 (100.0, M^+).

3-[{(2,6-Di(3,5-dimethylphenyl)phenyl)amino}methylene]-1,1,1,5,5,5-hexafluoropentane-2,4-dione (3c). ^{1}H NMR (400 MHz, C_6D_6, 25 °C): δ/ppm = 12.16 (d, $^3J_{HH}$ = 12.4 Hz, 1H, N*H*), 7.56 (d, $^3J_{HH}$ = 12.8 Hz, 1H, vinylic *H*C═C), 7.11 (d, $^3J_{HH}$ = 7.2 Hz, 2H, C*H* meta to NH), 6.84 (t, C*H* para to NH, 1H, $^3J_{HH}$ = 7.2 Hz), 6.77 (s, 4H, ortho C*H* of the CH_3 substituted aryl rings), 6.75 (s, 2H, para C*H* of the CH_3 substituted aryl rings), 2.12 (s, 12 H, 4 × CH_3). ^{13}C NMR (100 MHz, C_6D_6, 25 °C): δ/ppm = 181.17 (q, $^2J_{CF}$ = 38.3 Hz, CF_3CO), 175.23 (q, $^2J_{CF}$ = 34.7 Hz, CF_3CO), 160.13 (q, $^4J_{CF}$ = 5 Hz, vinylic *C*H), 139.32 (meta *C* of the CH_3 substituted aryl rings), 137.32 (*C* ipso to NH), 137.22 (ipso *C* of the CH_3 substituted aryl rings), 133.36 (*C* para to NH), 130.84 (*C* meta to NH), 130.24 (*C* ortho to NH), 127.05 (ortho *C* of the CH_3 substituted aryl rings), 122.52 (para *C* of the CH_3 substituted aryl rings), 117.02 (q, $^1J_{CF}$ = 286 Hz, *C*F_3CO), 116.91 (q, $^1J_{CF}$ = 291 Hz, *C*F_3CO), 102.73 (vinylic *C*═CH). ^{19}F NMR (376 MHz, C_6D_6, 25 °C): δ/ppm = −71.59 and −73.86 (CF_3CO). Anal. calcd (%) for $C_{28}H_{23}F_6NO_2$: C, 64.74; H, 4.46; N, 2.70. Found: C, 64.99; H, 4.57; N, 2.74. MS (*m*/*z*, %): 519 (35.5, M^+).

Synthesis of Complexes. Synthesis of the Pyridine Complexes 4a,b. 4 mL of diethyl ether and 1 mmol of pyridine were added to 0.1 mmol of ketoenamine (**3a,b**) and 0.1 mmol of [(tmeda)$NiMe_2$] at −50 °C. The temperature was raised to 0 °C, and the orange/red mixture was stirred for 30 min at this temperature. The solvent was removed in vacuo. **4a** was recrystallized from pentane at −30 °C. **4b** was purified by washing with pentane.

[κ²-*N*,O-3-[{(2,6-Diisopropylphenyl)imine}methyl]-1,1,1,5,5,5-hexafluoropent-3-ene-2-one-4-olato]methyl(pyridine)nickel(II) (4a). ^{1}H NMR (400 MHz, C_6D_6, 25 °C): δ/ppm = 8.20 (b, 2H, pyridine, C*H* ortho to N), 8.02 (s, 1H, vinylic C*H*═C), 7.03 (m, 3H, aryl), 6.56 (b, 1H, pyridine, C*H* para to N), 6.16 (b, 2H, pyridine, C*H* meta to N), 3.98 (sept, $^3J_{HH}$ = 6.4 Hz, 2H, ^{i}PrC*H*), 1.45 (d, $^3J_{HH}$ = 6.4 Hz, 6H, ^{i}Pr CH_3), 1.19 (d, $^3J_{HH}$ = 6.4 Hz, 6H, ^{i}Pr CH_3), −0.57 (s, 3H, Ni−CH_3). ^{13}C NMR (100 MHz, C_6D_6, 25 °C): δ/ppm = 177.5 (q, $^2J_{CF}$ = 34 Hz, CF_3CO,), 169.8 (q, $^2J_{CF}$ = 36 Hz, CF_3CO), 163.3 (vinylic *C*H═C), 151.2 (pyridine), 149.1 (ipso *C* of C_6H_3), 140.9 (ortho *C* of C_6H_3), 136.7 (pyridine), 127.3 (para *C* of C_6H_3), 124.6 (pyridine), 123.9 (meta *C* of C_6H_3), 119.2 (q, $^1J_{CF}$ = 291 Hz, *C*F_3), 117.6 (q, $^1J_{CF}$ = 291 Hz, *C*F_3), 105.7 (vinylic *C*═CH), 28.59 (^{i}Pr *C*H), 24.55 (^{i}Pr *C*H_3), 23.15 (^{i}Pr *C*H_3), −4.63 (s, Ni-*C*H_3). ^{19}F NMR (376 MHz, C_6D_6, 25 °C): δ/ppm = −70.95 and −71.54 (CF_3CO). Anal. calcd (%) for $C_{24}H_{26}F_6N_2NiO_2$: C, 52.68; H, 4.79; N, 5.12. Found: C, 52.72; H, 5.19; N, 5.16.

[κ²-*N*,O-3-[{(2,6-Di(3,5-bis(trifluormethyl)phenyl)phenyl)-imine}methyl]-1,1,1,5,5,5-hexafluoropent-3-ene-2-one-4-olato]-methyl(pyridine)nickel(II) (4b). ^{1}H NMR (400 MHz, C_6D_6, 25 °C): δ/ppm = 8.01 (s, 4H, ortho C*H* of the CF_3-substituted aryl groups), 7.88 (s, 2H, para C*H* of the CF_3-substituted aryl), 7.76 (b, 2H, pyridine, C*H* ortho to N), 7.48 (s, 1H, vinylic C*H*═C), 6.86−6.89 (m, 3H, aryl, C*H*s meta and para to N), 6.42 (b, 1H, pyridine, C*H* para to N), 6.09 (b, 2H, pyridine, C*H* meta to N), −0.74 (s, 3H, Ni−CH_3). ^{13}C NMR (100 MHz, C_6D_6, 25 °C): δ/ppm = 177.20 (q, $^2J_{CF}$ = 31 Hz, CF_3CO), 170.03 (q, $^2J_{CF}$ = 37 Hz, CF_3CO), 165.68 (vinylic *C*H═C), 149.68 (*C* ipso to N), 141.27 (ipso *C* of the CF_3-substituted aryl groups), 137.04 (pyridine, *C* para to N), 133.37 (*C* ortho to N), 132.44 (q, $^2J_{CF}$ = 33 Hz, meta *C* of CF_3-substituted aryl), 131.06 (*C* meta to N), 130.72 (ortho *C* of CF_3-substituted aryl), 127.41 (*C* para to N), 124.07 (pyridine, *C* meta to N), 123.74 (q, $^1J_{CF}$ = 272 Hz, *C*F_3 bound to aryl), 121.50 (para *C* of CF_3-substituted aryl), 120.79 (pyridine, *C* ortho to N), 118.41 (q, $^1J_{CF}$ = 282 Hz, CO*C*F_3), 116.90 (q, $^1J_{CF}$ = 291 Hz, CO*C*F_3), 105.82 (vinylic *C*═CH), −5.83 (Ni−CH_3). ^{19}F NMR (376 MHz, C_6D_6, 25 °C): δ/ppm = −63.16 (aryl C*F*$_3$), −71.81 (C*F*$_3$CO), −73.19 (C*F*$_3$CO). Anal. calcd (%) for $C_{34}H_{18}F_{18}N_2NiO_2$: C, 46.03; H, 2.05; N, 3.16. Found: C, 46.55; H, 2.44; N, 3.82.

Synthesis of the Phosphine Complex 5b. To a mixture of 50 μmol of **4b** and 50 μmol of PPh_3, 10 mL of diethyl ether were added at ambient temperature. After 10 min reaction time the solvent was removed in vacuo. An orange solid was obtained.

[κ²-*N*,O-3-[{(2,6-Di(3,5-bis(trifluormethyl)phenyl)phenyl)-imine}methyl]-1,1,1,5,5,5-hexafluoropent-3-ene-2-one-4-olato]-methyl(triphenylphosphine)nickel(II) (5b). ^{1}H NMR (400 MHz, C_6D_6, 25 °C): δ/ppm = 7.87 (m, 6H, aryl C*H* of the CF_3 substituted aryl groups), 7.73 (s, 1H, vinylic C*H*═C), 7.37 (b, 6H, ortho C*H* of PPh_3), 7.03 (b, 9H, meta and para C*H*s of PPh_3), 6.85−6.81 (m, 3H, N-aryl), −1.07 (s, 3H, Ni−CH_3). ^{13}C NMR (100 MHz, C_6D_6, 25 °C): δ/ppm = 177.85 (q, $^2J_{CF}$ = 37 Hz, CF_3CO), 169.80 (q, $^2J_{CF}$ = 39 Hz, CF_3CO), 165.23 (vinylic *C*H═C), 148.87 (*C* ipso to N), 141.35 (ipso *C* of the CF_3 substituted aryl rings), 133.98 (d, $^2J_{CP}$ = 10 Hz, ortho *C* of PPh_3), 133.47 (*C* ortho to N), 132.20 (q, $^2J_{CF}$ = 33 Hz, meta *C* of the CF_3 substituted aryl rings), 131.40 (*C* meta to N), 130.85 (para *C* of PPh_3), 130.75 (ortho *C* of the CF_3 substituted aryl rings), 129.36 (d, $^1J_{CP}$ = 46 Hz, ipso *C* of PPh_3), 128.60 (d, $^3J_{CP}$ = 10 Hz, meta *C* of PPh_3), 127.34 (para *C* to N), 123.84 (q, $^1J_{CF}$ = 272 Hz, *C*F_3 bound to aryl), 121.51 (para *C* of the CF_3 substituted aryl rings), 117.57 (q, $^1J_{CF}$ = 282 Hz, CO*C*F_3), 116.90 (q, $^1J_{CF}$ = 291 Hz, CO*C*F_3), 105.78 (vinylic *C*═CH), −6.68 (d, $^2J_{CP}$ = 35.2 Hz, Ni-*C*H_3). ^{31}P NMR (161 MHz, C_6D_6, 25 °C): δ/ppm = 31.61 (s, Ni−PPh_3). Anal. calcd (%) for $C_{47}H_{28}F_{18}NNiO_2P$: C, 52.74; H, 2.64; N, 1.31. Found: C, 51.90; H, 3.22; N, 1.66.

Polymerizations were carried out in a 300 mL stainless steel mechanically stirred (750 rpm) pressure reactor equipped with a heating/cooling jacket supplied by a thermostat controlled by a thermocouple dipping into the polymerization mixture. A valve controlled by a pressure transducer allowed for applying and keeping up a constant ethylene pressure. The required flow of ethylene, corresponding to ethylene consumed by polymerization, was monitored by a mass flow meter and recorded digitally. Prior to a polymerization experiment, the reactor was heated under vacuum to the desired reaction temperature for 30−60 min and then backfilled with argon.

For nonaqueous polymerizations, 95 mL of toluene were added to the reactor, and it was flushed and pressurized with ethylene three times. A solution of the catalyst precursor in 5 mL of toluene was injected via a Teflon cannula. The reactor was closed, and a constant ethylene pressure was applied. After the desired reaction time the reactor was rapidly vented and cooled to room temperature. The reaction mixture was stirred with an excess volume of methanol. The polymer was isolated by filtration, washed several times with methanol, and dried in vacuo.

For polymerization in aqueous emulsion, 80 mL of degassed water was introduced to the reactor, and ethylene pressure was applied in order to presaturate the solution. The catalyst precursor was dissolved in 2 mL of toluene and 0.1 mL of hexadecane (the latter functions as a hydrophobe). This toluene solution was added to 20 mL of an aqueous solution of 0.75 g of SDS. The biphasic mixture was homogenized under an argon atmosphere by means of an ultrasonic homogenizer (Bandelin HD2200 with KE76 tip, operated at 120 W, 2 min). The resulting miniemulsion was cannula-transferred to the aforementioned 300 mL pressure reactor. The pressure reactor was flushed with ethylene, and a constant ethylene pressure was then applied and the reaction mixture was brought rapidly to the desired temperature. After the specified reaction time, the reactor was vented and cooled. The emulsion was filtered through glass wool. No coagulate was observed. For determination of yields and for further polymer analysis a specified portion of the latex was precipitated by pouring into excess methanol. The polymer was washed three times with methanol and dried in vacuo at 50 °C.

X-ray Crystal Structure Determination of 3b. The data collection was performed at 100 K on a STOE IPDS-II diffractometer equipped with a graphite-monochromated radiation source (λ = 0.710 73 Å) and an image plate detection system. A crystal mounted on a fine glass fiber with silicon grease was employed. The selection, integration, and averaging procedure of the measured reflex intensities, the determination of the unit cell dimensions by a least-squares fit of the 2Θ values, data reduction, LP correction, and space group determination were performed using the X-Area software package delivered with the diffractometer. A semiempirical absorption correction was not performed. The structure was solved by direct methods (SHELXS-97), completed with difference Fourier syntheses, and refined with full-matrix least-squares using SHELXL-97 minimizing $w(F_o^2 - F_c^2)$.[2] Weighted *R* factor (*wR*) and the goodness of fit *S* are based on F^2; the conventional *R* factor (*R*) is based on *F*. All non-hydrogen atoms were refined with anisotropic displacement parameters. All scattering factors and anomalous dispersion factors are provided by the SHELXL-97 program. The hydrogen atom positions were calculated geometrically and were allowed to ride on their parent carbon atoms with fixed isotropic U_{11} = 0.02, except H27 which was located in the difference Fourier map and refined isotropically.

Acknowledgment. Financial support by the BMBF (project 03X5505) is gratefully acknowledged. We thank Ralf Thomann (Freiburg) for TEM analyses and Lars Bolk for GPC analyses. S.M. is indebted to the Fonds der Chemischen Industrie and to the Hermann-Schnell Foundation.

Supporting Information Available: Crystal structure data for compound **3b**. This material is available free of charge via the Internet at http://pubs.acs.org.

References and Notes

(1) (a) *Emulsion Polymerization and Emulsion Polymers*; Lovell, P. A., El-Aasser, M. S., Eds.; Wiley: Chichester, 1997. (b) Fitch, R. M. *Polymer Colloids: a Comprehensive Introduction*; Academic Press: San Diego, 1997. (c) *Wässrige Polymerdispersionen*; Distler, D., Ed.; VCH: Weinheim, 1999. (d) *Polymer Dispersions and Their Industrial Applications*; Urban, D., Takamura, K., Eds.; Wiley-VCH: Weinheim, 2002. (e) *Chemistry and Technology of Emulsion Polymerisation*; Herk, A. M., Ed.; Blackwell: Oxford, 2005.

(2) (a) Held, A.; Bauers, F. M.; Mecking, S. *Chem. Commun.* **2000**, 301. (b) Bauers, F. M.; Mecking, S. *Macromolecules* **2001**, *34*, 1165. (c) Bauers, F. M.; Mecking, S. *Angew. Chem.* **2001**, *113*, 3112; *Angew. Chem. Int. Ed.* **2001**, *40*, 3020. (d) Bauers, F. M.; Chowdhry, M. M.; Mecking, S. *Macromolecules* **2003**, *36*, 6711. (e) Bauers, F. M.; Thomann, R.; Mecking, S. *J. Am. Chem. Soc.* **2003**, *125*, 8838. (f) Zuideveld, M. A.; Wehrmann, P.; Röhr, C.; Mecking, S. *Angew. Chem.* **2004**, *116*, 887; *Angew. Chem. Int. Ed.* **2004**, *43*, 869. (g) Kolb, L.; Monteil, V.; Thomann, R.; Mecking, S. *Angew. Chem., Int. Ed.* **2005**, *44*, 429; *Angew. Chem.* **2005**, *117*, 433. (h) Monteil, V.; Wehrmann, P.; Mecking, S. *J. Am. Chem. Soc.* **2005**, *127*, 14568. (i) Göttker gen.

Schnetmann, I.; Korthals, B.; Mecking, S. *J. Am. Chem. Soc.* **2006**, *128*, 7708.
(3) (a) Tomov, A.; Broyer, J.-P.; Spitz, R. *Macromol. Symp.* **2000**, *150*, 53. (b) Soula, R.; Novat, C.; Tomov, A.; Spitz, R.; Claverie, J.; Drujon, X.; Malinge, J.; Saudemont, T. *Macromolecules* **2001**, *34*, 2022. (c) Soula, R.; Saillard, B.; Spitz, R.; Claverie, J.; Llaurro, M. F.; Monnet, C. *Macromolecules* **2002**, *35*, 1513.
(4) Reviews: (a) Mecking, S.; Held, A.; Bauers, F. M. *Angew. Chem.* **2002**, *114*, 564; *Angew. Chem. Int. Ed.* **2002**, *41*, 544. (b) Mecking, S.; Claverie, J. In *Late Transition Metal Polymerization Catalysis*; Rieger, B., Baugh, L. S., Kacker, S., Striegler, S., Eds.; Wiley-VCH: Weinheim, 2003; pp 231−278. (c) Mecking, S. *Colloid Polym. Sci.*, in press.
(5) (a) Younkin, T. R.; Connor, E. F.; Henderson, J. I.; Friedrich, S. K.; Grubbs, R. H.; Bansleben, D. A. *Science* **2000**, *287*, 460−462. (b) Wang, C.; Friedrich, S.; Younkin, T. R.; Li, R. T.; Grubbs, R. H.; Bansleben, D. A.; Day, M. W. *Organometallics* **1998**, *17*, 3149−3151.
(6) Soula, R.; Broyer, J. P.; Llauro, M. F.; Tomov, A.; Spitz, R.; Claverie, J.; Drujon, X.; Malinge, J. Saudemont, T. *Macromolecules* **2001**, *34*, 2438−2442.
(7) Zhang, L.; Brookhart, M.; White, P. S. *Organometallics* **2006**, *25*, 1868−1874.
(8) Hristov, I. H.; DeKock, R. L.; Anderson, G. D. W.; Göttker-Schnetmann, I.; Mecking, S.; Ziegler, T. *Inorg. Chem.* **2005**, *44*, 7806−7818.
(9) Zhu, S. Z.; Xu, B.; Zhang, J. *J. Fluorine Chem.* **1995**, *74*, 167−170.
(10) Schmid, M.; Eberhardt, R.; Klinga, M.; Leskelä, M.; Rieger, B. *Organometallics* **2001**, *20*, 2321−2330.
(11) *Handbook of Chemistry and Physics*, 64th ed.; CRC Press: Boca Raton, FL, 1984.
(12) Kaschube, W.; Poerschke, K. R.; Wilke, G. *J. Organomet. Chem.* **1988**, *355*, 525−32.
(13) Connor, E. F.; Younkin, T. R.; Henderson, J. I.; Waltman, A. W.; Grubbs, R. H. *Chem. Commun.* **2003**, *18*, 2272−2273.
(14) Bastero, A.; Kolb, L.; Wehrmann, P.; Bauers, F.; Göttker-Schnetmann, I.; Monteil, V.; Thomann, R.; Chowdhry, M.; Mecking, S. *Polym. Mater. Sci. Eng.* **2004**, *90*, 740−741.
(15) Klabunde, U.; Ittel, S. D. *J. Mol. Catal.* **1987**, *41*, 123−134.
(16) Mecking, S.; Monteil, V.; Huber, J.; Kolb, L.; Wehrmann, P. *Macromol. Symp.* **2006**, *236*, 117−123.
(17) (a) Randall, J. C. *J. Macromol. Sci., Rev. Macromol. Chem. Phys.* **1989**, *C29*, 201−317. (b) Axelson, D. E.; Levy, G. C.; Mandelkern, L. *Macromolecules* **1979**, *12*, 41−52.

MA061804N